Hypocentre estimation of induced earthquakes in Groningen

Spetzler, Jesper; Dost, Bernard

Important note
To cite this publication, please use the final published version (if applicable).
Please check the document version above.

Hypocentre estimation of induced earthquakes in Groningen

Jesper Spetzler[1,2] and Bernard Dost[1]

[1]*Royal Netherlands Meteorological Institute, P.O. Box* 201, *NL-3730 AE De Bilt, The Netherlands. E-mail:* *jesper.spetzler@knmi.nl*
[2]*Department of Geoscience and Engineering, Delft University of Technology, P.O. Box* 5048, *NL-2600 GA Delft, The Netherlands*

SUMMARY
Induced earthquakes due to gas production have taken place in the province of Groningen in the northeast of The Netherlands since 1986. In the first years of seismicity, a sparse seismological network with large station distances from the seismogenic area in Groningen was used. The location of induced earthquakes was limited by the few and wide spread stations. Recently, the station network has been extended significantly and the location of induced earthquakes in Groningen has become routine work. Except for the depth estimation of the events. In the hypocentre method used for source location by the Royal Netherlands Meteorological Institute (KNMI), the depth of the induced earthquakes is by default set to 3 km which is the average depth of the gas-reservoir. Alternatively, a differential traveltime for *P*-waves approach for source location is applied on recorded data from the extended network. The epicentre and depth of 87 induced earthquakes from 2014 to July 2016 have been estimated. The newly estimated epicentres are close to the induced earthquake locations from the current method applied by the KNMI. It is observed that most induced earthquakes take place at reservoir level. Several events in the same magnitude order are found near a brittle anhydrite layer in the overburden of mainly rock salt evaporites.

Key words: Body waves; Computational seismology; Induced seismicity.

1 INTRODUCTION

Induced earthquakes due to gas production have occurred in the North of the Netherlands over the last 30 yr (Dost & Haak 2007; Bourne *et al.* 2015). The first events were felt near small gas fields in production, followed by activity that could be related to the Groningen gas field, one of the largest onshore gas fields in the world. Seismicity rate of the Groningen field gradually increased over the years until 2003. Since then activity rate increased more strongly, coinciding with an increase in annual gas production.

Observed magnitudes of the induced earthquakes in Groningen are usually in the lower range of the Richter scale ($0.5 < M_L < 3.0$) except for a few stronger events in 2006 and 2012. An event with magnitude 3.5 took place on 2006 August 8, while the largest event recorded was the magnitude 3.6 on 2012 August 16 (Dost & Kraaijpoel 2013). The epicentres of these two events were close to the small town of Huizinge. Many people were surprised by the sudden feeling of strong ground motion and a substantial amount of building damage was reported, due to the shallow depth, around 3 km, of the events

In the year 1995, the KNMI realized a sparse regional borehole network with average distance between stations of 20 km. The network geometry, covering a heterogeneous shallow crustal structure, limited the resolution of the location of induced earthquakes to 0.5–1 km. The network was gradually extended over time, with the aim of covering a larger region. After the M3.6 event in 2012, it

was decided to increase the number of stations significantly with the result that currently the average interstation distance is reduced to 3–4 km.

Originally, the KNMI used the traditional *P*- and *S*-wave arrival time difference method to locate induced earthquakes with the sparse network using the hypocentre method (Aki & Richards 1980) and an average 1-D velocity model for the region. It has proven difficult to resolve the depth of the events, which is by default set to 3 km, the average depth of the gas reservoir in Groningen. Nevertheless, a good estimate of the depths of the induced earthquakes in Groningen would add valuable information that is useful for hazard analysis (Bommer *et al.* 2016).

In the year 2013, two deep downhole arrays were installed in the most active region near the village of Loppersum with the aim to record microseismicity at reservoir level and determine the depth extend of the seismic activity. Arrival time inversion using a grid search location algorithm (Pickering 2015) was applied and it was concluded that all events processed occurred at a depth of the reservoir. Since the deep arrays only cover a small region of the Groningen field and larger events saturate the geophones used, it is a challenge to improve the depth estimation using the improved shallow borehole network set-up in Groningen.

A popular method to relocate earthquakes is the double difference method (Waldhauser & Ellsworth 2000; Zhang & Thurber 2006). In the double difference method, traveltime differences of recorded waveforms at one station for several earthquakes are used to

reposition the epicentres. A different method, more suitable for real-time and off-line relocation of individual events is the differential traveltime method where waveforms from one specific event are measured at several stations (Font *et al.* 2004; Lomax 2005; Satriano *et al.* 2008; Theunissen *et al.* 2012). The traveltime shift of the recorded waves between stations is used to find the focus of the earthquake. In Lomax (2005) and Theunissen *et al.* (2012), the differential traveltime method between stations is known as equal differential time EDT. We adopt the EDT abbreviation for our approach in this paper. The differential traveltime approach is insensitive to the depth-origin time trade-off. On the contrary, the hypocentre method is based on the minimization of traveltime residuals, where information about the origin time (e.g. related to the depth of the event) is important.

The hypocentre method for *P*-wave arrivals (Lienert *et al.* 1986) is implemented in the automatic routine for source location at the KNMI. The addition of stations to the network and the use of a detailed local velocity model did not lead to a more accurate depth estimation of induced earthquakes in Groningen. The event depth is still by default set to 3 km.

In the present paper, we will explore how the rapidly growing data set with picked *P*-wave arrivals for induced events in Groningen can best be used to determine reliable depth estimates of induced events in the region. Generally, picked *S*-waves are not used in the automatic hypocentre solution since the first arrival is *S*-phases are difficult and often impossible to estimate. The extended station network guarantees that an event will always be relatively close to at least three stations. In addition, the producer (Nederlandse Aardolie Maatschappij, NAM) of the gas field has made available a detailed 3-D elastic model of the complex subsurface structure of Groningen. Theunissen *et al.* (2012) conclude that the more accurate the velocity model is the better the estimation of the hypocentre of an event. Altogether, more data and accurate information about the complex heterogeneous of Groningen is becoming available.

We will give an outline of the seismological station network and the geological model in Groningen. The slightly adapted differential traveltime method for *P*-waves is introduced. A 2-D synthetic experiment with two stations over a constant half-space velocity model is used to illustrate how to estimate the hypocentre of an event. Results of the differential traveltime method applied on earthquake data from 2014 to July 2016 are presented and compared to the KNMI hypocentre solutions. Finally, conclusions are drawn.

2 SEISMOLOGICAL NETWORK

A borehole network of geophones was installed in 1995 with the aim to detect and locate induced seismicity in the North of the Netherlands. The network was intended to cover an area of 60 × 80 km and designed to record all events in the region of magnitude 1.5 and larger. The station separation was on average 20 km and due to the sampling of a heterogeneous upper crust, location accuracy was limited to 0.5–1 km in the horizontal plane. The resolution in the vertical plane was even more limited, at least 1–2 km. In 2014 and 2015 the network was extended over the Groningen area, resulting in an average station separation of 4 km, which opened the possibility to use detailed velocity models and new location algorithms.

The monitoring network developed over time from 11 borehole geophone stations in 1996 to 15 stations in and outside of Groningen with the addition of 17 accelerometers deployed at the surface until 2014. In the year 2015, another 60 borehole stations distributed equally over Groningen were added to the network. The location

threshold value of the network has been reduced from 2.3 in 1991 to 1.5 in 2008 and currently to about 0.5.

The current network of seismological stations by February 2016 is illustrated in Fig. 1. Each station location is indicated with a triangle. The stations are either three-component instruments in four-level boreholes (white triangle), accelerometers (dark grey triangle) and broad-band stations (black triangle). The four-level boreholes are 200 m deep wells with a three-component instrument at −200, −150, −100 and −50 m. The deepest instruments have the best S/N ratio. An accelerometer is placed at the surface of each new borehole. Additional accelerometers at the surface have been installed at other locations. A plot with an event gather with waveform data and first arrival time picks of the M2.4 Froombosch event on 2016 February 25 is shown in Fig. 2. In general, the first arrival times for *P*-waves (indicated with dark grey lines in the figure) are always picked and used in the automatic location method. Traveltime picking is done for the first arriving *S*-waves only if the events are clearly observable. *S*-wave picks are never used in the automatic routine, but may later be added to the data base of traveltimes and used in a relocation of the original epicentre.

3 GEOLOGICAL SETTING OF GRONINGEN

One of the largest onshore gas fields is located in the province of Groningen in the northeast of The Netherlands. Fig. 1 shows the location of Groningen in The Netherlands (Dost & Haak 2007; Bourne *et al.* 2015). The surface area of Groningen is about 1000 km². A lithological setting of sedimentary layers dominates the geology of the area (Dalfsen *et al.* 2006; Duin *et al.* 2006; van Gent *et al.* 2011; NLog). The black dotted lines in Fig. 1 indicate the positions of two cross-sections of the stratigraphy in Groningen. The two cross-sections for north–south and east–west directions of the velocity field are shown in Fig. 3. The Dutch RD coordinate system (description in English: https://translate.google.nl/translate?hl=en&sl=nl&u=https://nl.wikipedia.org/wiki/Rijksdriehoeksco%25C3%25B6rdinaten&prev=search, or in Dutch: Rijksdriehoeksstelsel, http://www.kadaster.nl/web/Themas/Registraties/Rijksdriehoeksmeting/Rijksdriehoeksstelsel.htm) is used in all cross-section figures. This specific coordinate system gives the geodetic coordinates for European Netherlands and is used in official national maps. The origin of the RD coordinates system is in the spire of Our Lady Tower (Long John) in Amersfoort (52°9′19″N, 5°23′14″). The cross-sections of the velocity field in Fig. 3 have been extracted from a 3-D detailed elastic model for Groningen. A vast geophysical data set of 3-D seismic reflection data and several deep well log data going down to the carboniferous layer below the gas reservoir were used to produce the 3-D elastic model. NAM contributed to this work with the 3-D elastic model.

The stratigraphic setting is explained from the surface and down to the underburden below the gas-filled reservoir. The top layer is the North Sea (NS) group containing clays, silts and sandstone. The thickness of the NS group varies between 600 and 1000 m. The NS layer is subdivided into an upper and lower part. The transition from upper NS to lower NS is at 400 m depth. The velocity in upper NS is significantly lower than in lower NS. The next layer is the Chalk (CK) group which is made of mainly limestone. The thickness of the Chalk layer is between 500 and 800 m. A sequence of three thinner sedimentary layers are found below the Chalk group. These layers are the Rijnland (RN) group, the Altena (AL) group
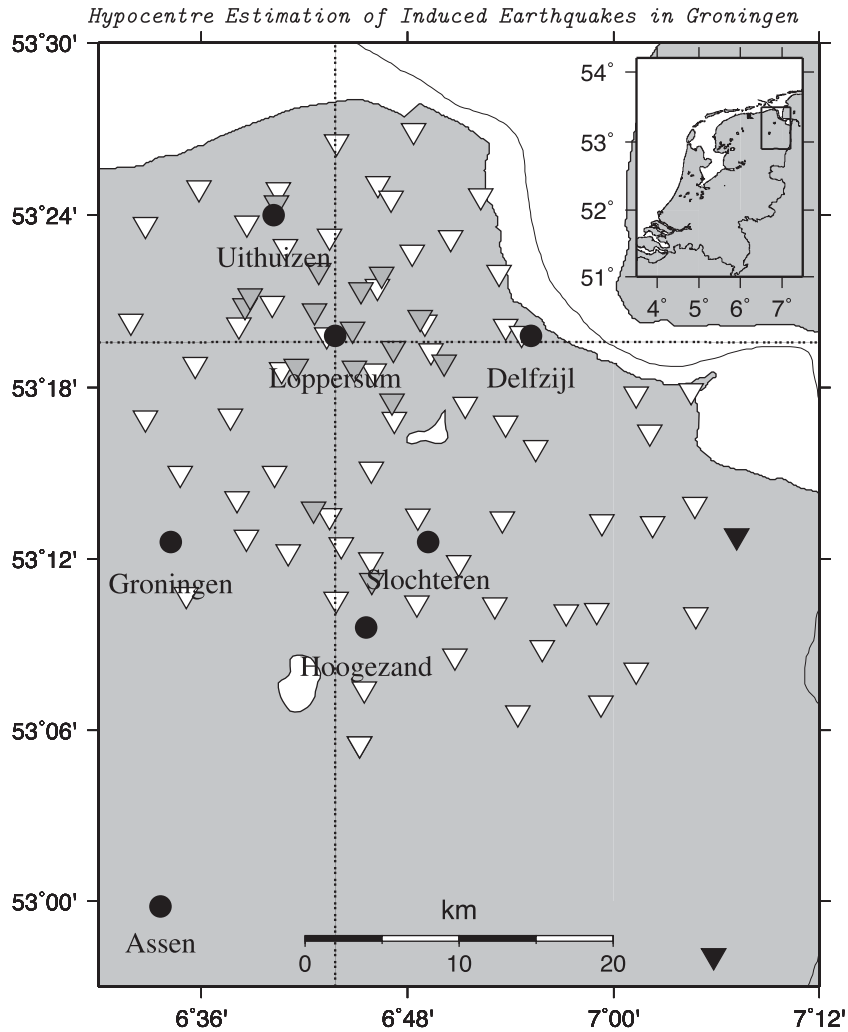
Figure 1. Location of the province of Groningen in the north–east of the Netherlands. Larger cities in Groningen are indicated with a circle, while locations with different instruments are shown with triangles. White triangles indicate borehole stations, dark grey triangles show old surface accelerometers and black triangles are for broad-band stations. The locations of the cross-sections in Fig. 3 are illustrated with the black dotted lines.
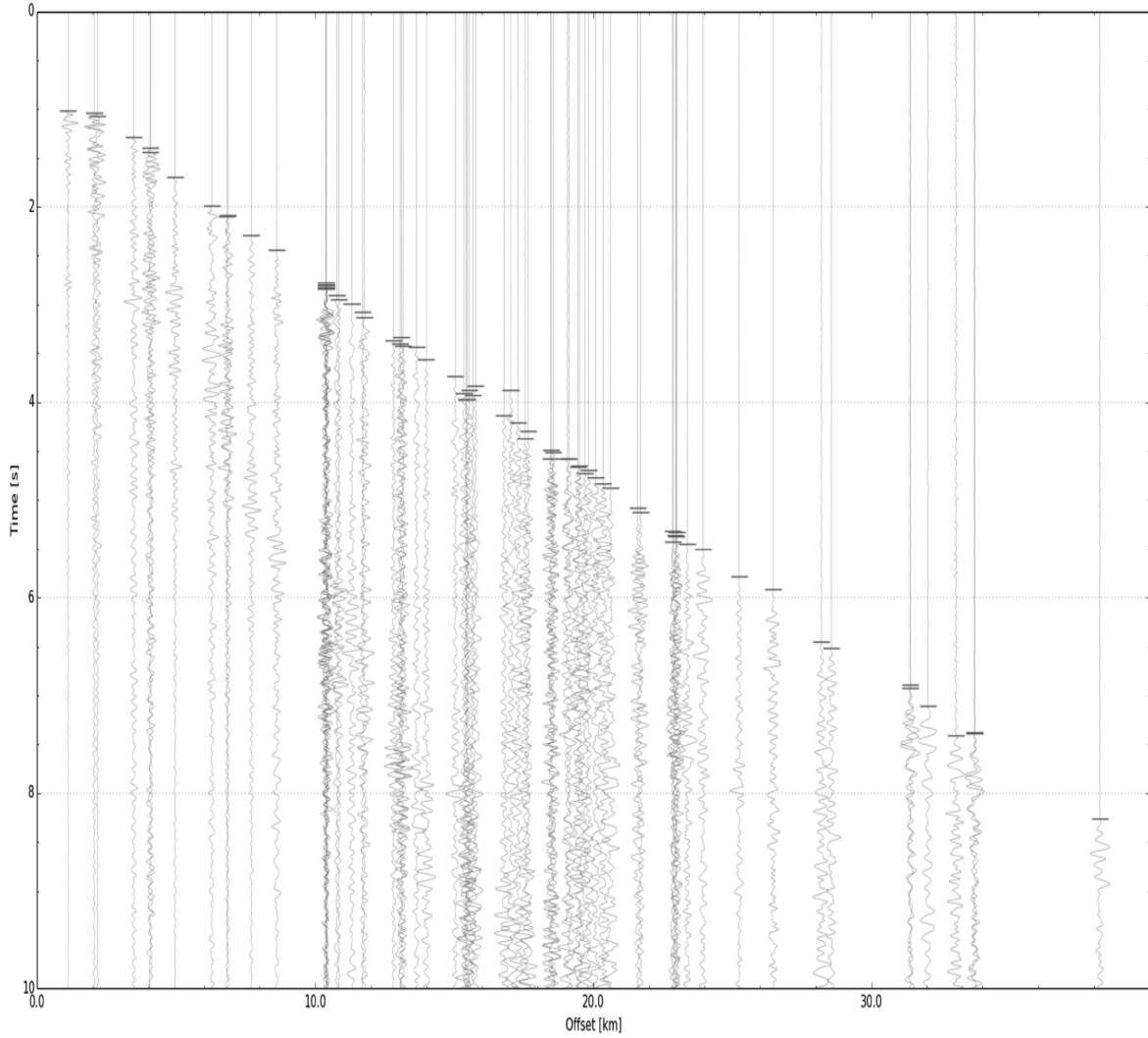
and the Trias (TR) group. The Zechstein (ZE) group is a layer of rock salt evaporites. In general, the Zechstein layer is referred to as the impermeable salt layer above the gas reservoir. The Zechstein layer is thickest in the central area of the gas field near Loppersum (see Fig. 1) and tends to get thinner at the north, south and east flanks of Groningen. Note the lateral variations in the Zechstein layer with horst and graben structures. To complicate matters, two thin layers of anhydrite (Dino loket) are present in the Zechstein group: One anhydrite layer in the upper section of Zechstein and another one right above the gas reservoir (van Gent *et al.* 2011). These two stiff, brittle layers in the soft Zechstein group give rise to strong reflected and refracted waves. The reservoir (RO) is composed of a porous sandstone in the upper-Rotliegend group. The depth of the gas reservoir is on average 3 km, but varies laterally over Groningen. The sedimentary layer below the Rotliegend group is part of the Limburg group from the late carboniferous age. The carbon layer (DC) is the rock source for the gas which has been pushed upward into the Rotliegend layer and is prevented from migrating further upward by the impermeable Zechstein group. Faults are present mainly in the Rotliegend gas reservoir layer due to extensional stress conditions. The faults do not extend vertically into the Zechstein layer because of the ductile and malleable behaviour

of rock salt under high pressure. The faults are generally aligned NW-SE (Kraaijpoel & Dost 2013). Several of the faults have been reactivated during the production of gas in Groningen in the past 40 yr.

4 DIFFERENTIAL TRAVELTIME METHOD

The concept of the differential traveltime for *P*-waves method for source location is illustrated in Fig. 4. Lomax (2005) and Theunissen *et al.* (2012) apply the same principle in the construction of their source location method. An earthquake is located at the position **s**. The seismological network stations record the earthquake. For example, the two stations in Fig. 4 are at positions $\mathbf{r}_1$ and $\mathbf{r}_2$. Let the unknown origin time for an earthquake be written as T_0. In general, the origin time for an earthquake can be determined after the focus of the earthquake has been estimated. The recorded arrival time for a wave to travel from the source position **s** to receiver $\mathbf{r}_1$ is given by

$$T(\mathbf{r}_1, \mathbf{s}) = T_0 + \int_{\text{ray}} \frac{1}{V(\mathbf{r})} dr, \qquad (1)$$

Network: NL [HHZ] - (72 traces / 2016-02-25T22:26:30.899999)

Figure 2. Example of recorded waveforms and an observed traveltime curve for an induced earthquake near Froombosch on 2016 February 25.

where the integration along the ray path in a heterogeneous velocity field V between the earthquake $\mathbf{s}$ and station $\mathbf{r}_1$ yields the traveltime of the wave (Aki & Richards 1980). Similarly for receiver $\mathbf{r}_2$, the recorded arrival time is given by

$$T(\mathbf{r}_2, \mathbf{s}) = T_0 + \int_{\mathrm{ray}} \frac{1}{V(\mathbf{r})} dr. \tag{2}$$

To eliminate the unknown origin time, the recorded arrival time in eq. (1) is subtracted from eq. (2). The differential traveltime is obtained as

$$\Delta T(d) = T(\mathbf{r}_2, \mathbf{s}) - T(\mathbf{r}_1, \mathbf{s}), \tag{3}$$

where $d = \|\mathbf{r}_2 - \mathbf{r}_1\|$ is the epicentral distance between the two receivers at the same depth. Expression (3) demonstrates that the differential traveltime method is insensitive to the depth-origin time trade-off.

To find the focus of an earthquake, an objective function is defined. The earthquake location is determined by minimizing the objective function. We follow the EDT approach by Font *et al.* (2004), Lomax (2005) and Satriano *et al.* (2008). The observed differential traveltimes ΔT_{obs} between stations in eq. (3) are compared with the calculated traveltime differences ΔT_{calc} for an earthquake

at an arbitrary depth. The advantage of working with time shifts between two stations is not only that the origin time of the earthquake cancels out (Satriano *et al.* 2008), but also that errors due to inaccuracy in the reference velocity model and modelling limitations and artefacts may be eliminated. The difference between the observed − and calculated differential traveltimes are squared and summed up for all station pairs. Two additional steps are carried out. (1) The sum of squared differential traveltimes is multiplied by the depth z to enhance the depth resolution of the objective function. This step is not a strict requirement, but is helpful to emphasize the depth resolution. (2) The average objective function is calculated by dividing with the number N of available station pairs to account for the fact that not all stations have an epicentral distance within the maximum distance of a pre-calculated traveltime function. Hence, the depth-dependent objective function $L(z)$ is given by

$$L(z) = \frac{z}{N} \sum_i^N (\Delta T_{\mathrm{obs}} - \Delta T_{\mathrm{calc}})^2. \tag{4}$$

The addition of the linear depth term z is in the SI-unit metre and the averaging over the number of stations pairs is specifically introduced in this paper. However, the summation of the differential

(a)

(b)
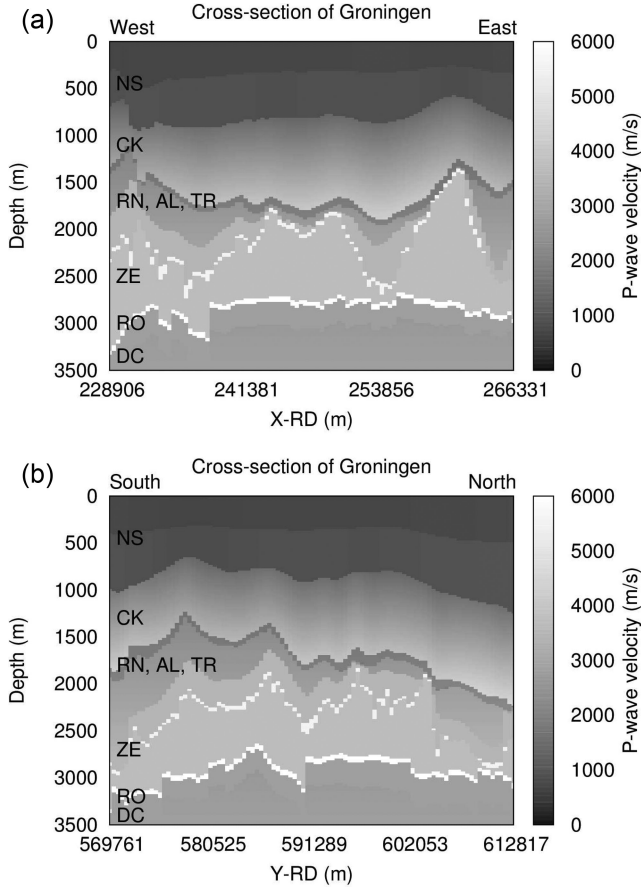
Figure 3. The 3-D velocity field of Groningen. The crossing point for the two perpendicular cross-sections is located in the central field as it is illustrated with black dotted lines in Fig. 1. (a) West–east cross-section. (b) South–north cross-section. The scaling factor between the horizontal and vertical direction is 13. Data courtesy of NAM.

traveltime residuals over all available station pairs is as well applied by Lomax (2005) and Theunissen *et al.* (2012). The earthquake focus is obtained at the minimum point of the objective function in eq. (4).

The maximum number of station pairs can be calculated from the number of available stations denoted N_r. The number of combinations of station pairs (each pair counting one time) is given by

$$N = \frac{N_r!}{2(N_r - 2)!} \qquad (5)$$

Expression (5) is valid for two or more stations. For example, three stations results in three station pairs, four stations yield six combinations and so on.

For an example of the use of the objective function in eq. (4), consider a homogeneous half-space model with the constant velocity $v = 2000 \text{ m s}^{-1}$. An illustration of the setup of the earthquake and stations can be found in Fig. 5. The earthquake is located at 7000 m to the right of station $\mathbf{r}_1$ and depth $h = 2600$ m. For convenience, station $\mathbf{r}_1$ and $\mathbf{r}_2$ have the surface coordinates 0 m and 11 000 m, respectively. The time for the recording of the earthquake at station $\mathbf{r}_1$ is calculated with eq. (1), hence for the homogeneous velocity field with $x = 7000$ m,

$$T(\mathbf{r}_1, \mathbf{s}) = T_0 + \frac{\sqrt{x^2 + h^2}}{v} = T_0 + 3.734 \text{ s}. \qquad (6)$$
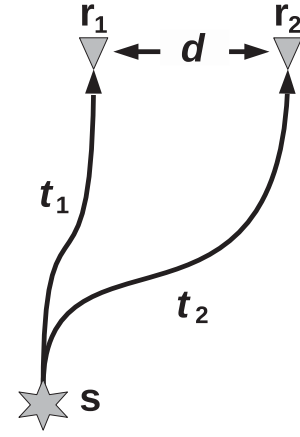
Figure 4. Concept of the differential time for *P*-phase method. Body waves propagate from an earthquake indicated with the grey star to the two receivers $\mathbf{r}_1$ and $\mathbf{r}_2$. The receivers are illustrated with the grey triangles. The epicentral distance between the receivers is denoted by d. The traveltime for the waves is t_1 and t_2 for the first and second stations, respectively.
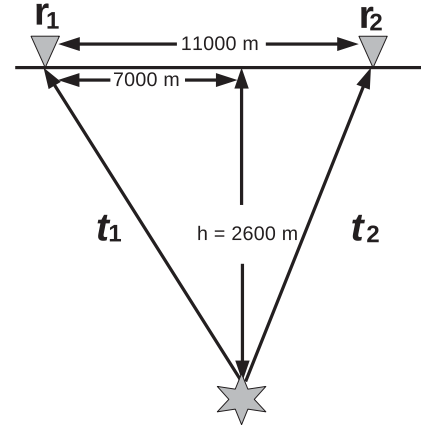
Figure 5. Synthetic example of depth estimation of an earthquake. The arrival times t_1 and t_2 of the propagating waves from the earthquake are recorded at the two stations $\mathbf{r}_1$ and $\mathbf{r}_2$, respectively.

In similar veins, the recording time of the earthquake at station $\mathbf{r}_2$ equals

$$T(\mathbf{r}_2, \mathbf{s}) = T_0 + \frac{\sqrt{(L - x)^2 + h^2}}{v} = T_0 + 2.385 \text{ s}, \qquad (7)$$

where $L - x = 4000$ m. The observed differential traveltime between station $\mathbf{r}_1$ and $\mathbf{r}_2$ equals

$$\Delta T(d = 11\,000 \text{ m}) = T(\mathbf{r}_1, \mathbf{s}) - T(\mathbf{r}_2, \mathbf{s}) = 1.349 \text{ s}. \qquad (8)$$

Note that the unknown origin time of the earthquake is eliminated in the equation above. Combining the expressions for the traveltimes in eqs (6) and (7) and the observed differential traveltime in eq. (8), we explicitly obtain for the homogeneous velocity field the objective function

$$L(x, z) = z \left[\Delta T(d = 11\,000 \text{ m}) - \left(\frac{\sqrt{x^2 + z^2}}{v} - \frac{\sqrt{(L - x)^2 + z^2}}{v} \right) \right]^2, \qquad (9)$$

where an arbitrary earthquake is located at (x, z). A global search method applied on the objective function results in the minimum

(a)

(b)
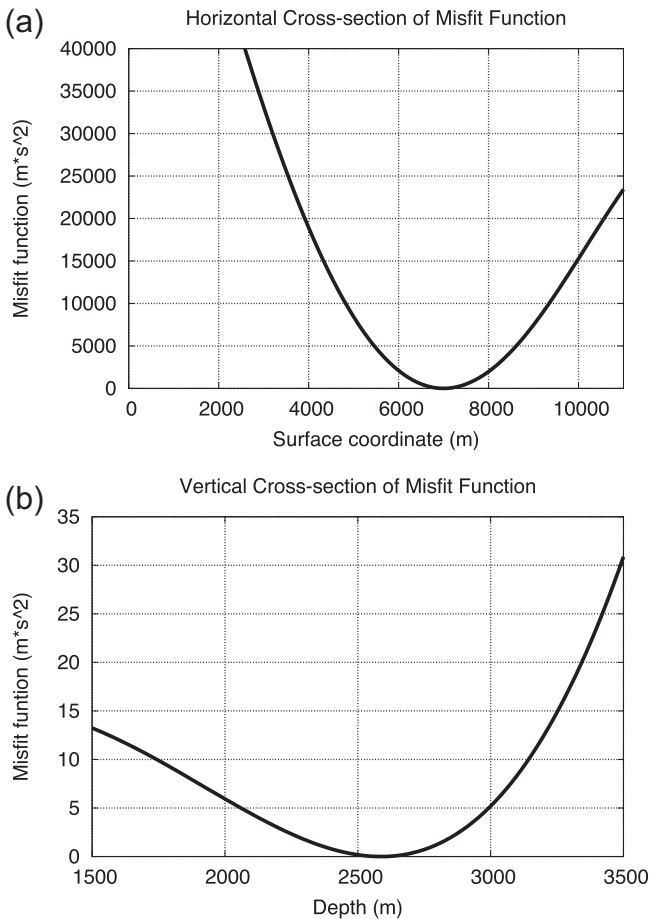
**Figure 6.** Misfit function for the synthetic example with a homogeneous velocity field. (a) The horizontal cross-section for fixed depth value, $h = 2600$ m. (b) The vertical cross-section for fixed value of the surface coordinate, $x = 7000$ m.

point at the coordinate point (7000 m, 2600 m) which is the theoretical location of the earthquake in the synthetic experiment. The horizontal and vertical cross-sections of the objective function are shown in Fig. 6. Theunissen *et al.* (2012) carry out an extensive sensitivity analysis of the EDT method in terms of an inadequate velocity model and a poor station coverage. It is concluded in Theunissen *et al.* (2012) that the EDT method in most cases does a much better job in estimating the focus of an event than the hypocentre method (Lienert *et al.* 1986). The hypocentre method tends to overestimate the depth parameter because of the depth-origin time trade-off.

The presented synthetic example is constructed for a 2-D half-space model and only two stations are strictly required to estimate the focus of an event. The induced earthquakes in Groningen take place in a 3-D regional area. Like the general requirements for seismological focus estimation using the difference between *P*-wave and *S*-wave traveltimes (Aki & Richards 1980), at least three stations must be available in the EDT method. Estimation of the origin time is not the scope of this paper, but is of course possible to estimate.

The KNMI applies the hypocentre method (Lienert *et al.* 1986) for the location of induced earthquakes in Groningen. The hypocentre method is strongly dependent on the depth-origin time trade-off. According to Lienert *et al.* (1986), the origin time is defined as the mean arrival times minus the mean traveltimes. The traveltimes can only be calculated assuming a given depth of an event. Second, the 1-D velocity profile in Fig. 7 for the KNMI hypocentre
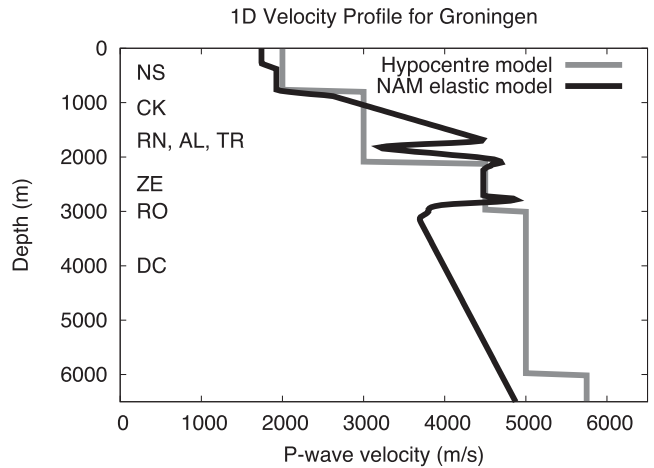

Figure 7. Example of the 1-D *P*-wave velocity profile (black solid line) that is used to calculate depth-dependent traveltime curves. The grey solid line shows the 1-D velocity model applied in the hypocentre method.

method is an average model that is representative for the northern part of the Netherlands. The detailed structures of the overburden, the Zechstein group and Carboniferous group in Groningen are not well-represented in the hypocentre velocity model. traveltime functions based on this velocity structure are calculated with a tau-p method for epicentral distances to 120 km. Modifications of the 1-D velocity model in the hypocentre method did not improve the depth resolution.

5 METHODOLOGY FOR FOCUS ESTIMATION OF INDUCED EARTHQUAKES IN GRONINGEN

Induced earthquakes in Groningen are believed to be caused by a reactivation of existing faults due to compaction after the production of gas was initiated in the late 1960. To get an idea about how compressional and shear wave energy propagate in the Zechstein group dominated subsurface, a full elastic waveform study was carried out. Naturally, waves in the Groningen subsurface propagate in a 3-D half-space. However, the waveform modelling experiment was limited to 2-D media to reduce calculation time. The main difference in results between 2-D and 3-D waveform modelling is the behaviour of the geometrical spreading factor (Aki & Richards 1980; Snieder 2004) which affects the amplitude of wavefields. Hence, it is expected that amplitude effects may be different in observed data compared to synthetic waveforms in the 2-D full elastic wave modelling experiment. On the other hand, the phase information in the propagating elastic waves will be identical for 2-D and 3-D media.

The east–west cross-section in Fig. 3 was used as elastic model input in a 2-D finite-difference (FD) program (Robertson *et al.* 1994). The dimensions of the input model was 30 km horizontally and 10 km vertically. The central frequency in the FD modelling was set to 5 Hz which is equivalent to the dominant frequency of recorded induced earthquake data in the shallow boreholes in Groningen. A *Q*-value equal to 200 is representative for Groningen (Bommer *et al.* 2016) and was accordingly applied. The top boundary acts as a free surface. The grid size and temporal step length were adjusted to satisfy the Courant number (Robertson *et al.* 1994). A proper taper was implemented to reduce boundary reflections.
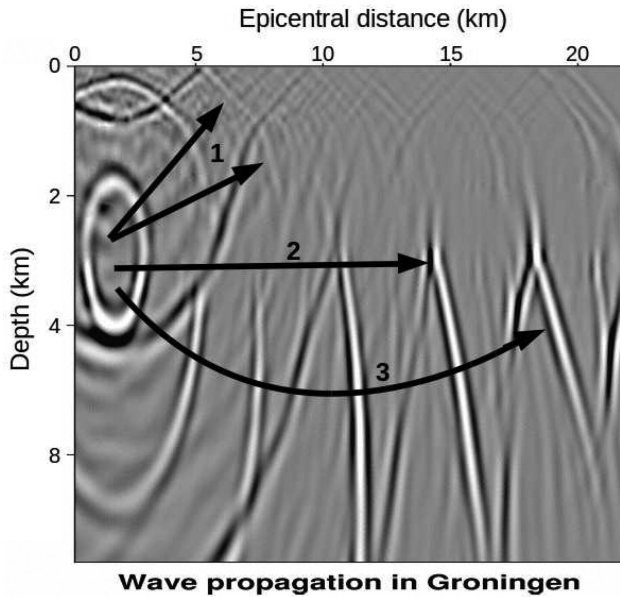
Figure 8. Illustration of principle components of wave propagation in the complex Groningen subsurface. The source depth is 3 km.

A simulation of wave propagation in the Groningen subsurface is shown in Fig. 8 for a source at 3 km depth. The epicentral distance from the surface coordinate of the source is given in kilometres. Three dominant wave directions are observed. There is the direct wavefield (**1**) from the source towards the surface. The reservoir has a lower velocity compared to the Zechstein group and the Carboniferous layer and therefore acts as a strong wave guide giving rise to high amplitude waves (**2**). The underburden with the Carbon group is characterized by a linear gradient velocity. Wave energy propagating downwards (**3**) from the source will be redirected upward in the underburden and eventually be recorded at the shallow borehole stations close to the surface. Finally, internal multiples and interface conversions between compressional and shear wave energy are part of the propagating wavefield. These latter waves will have longer traveltimes due to the longer propagation paths and will have low amplitudes because of reflection/transmission effects at layer interfaces (Aki & Richards 1980; Kennett 1993; Kraaijpoel & Dost 2013). Especially, free surface reverberations are clearly visible in the upper part of the waveform snapshots in Fig. 8.

The EDT method would be rather time inefficient if the traveltime for a wavefield from a given source depth to a station was repeatedly calculated in a 3-D heterogeneous velocity model. Instead to speed up calculations, a local 1-D velocity profile is used to compute a series of traveltime functions for a wide range of source depths and epicentral distances. A 1-D velocity profile with the RD-coordinate point (Dutch coordinate system: 246 877, 593 444) from the Loppersum area (i.e. seismic active zone) was extracted from the 3-D elastic model. The velocity profile is shown in Fig. 7. A narrow moving average window has been used to smooth the velocity profile. Still, the fine structures of the Groningen subsurface are well-preserved. The velocity smoothing was introduced to facilitate the calculation of traveltime functions by means of a ray tracing algorithm. A direct solver for the eikonal equation is the workhorse to calculate ray paths for a given source depth and epicentral distance to a station. The traveltime between the source and station is calculated using the path integral in eq. (1). Calculated ray paths and traveltime curves are shown in Fig. 9 and 10, respectively, for source depths at 2500, 3000 and 3500 m. In general, the
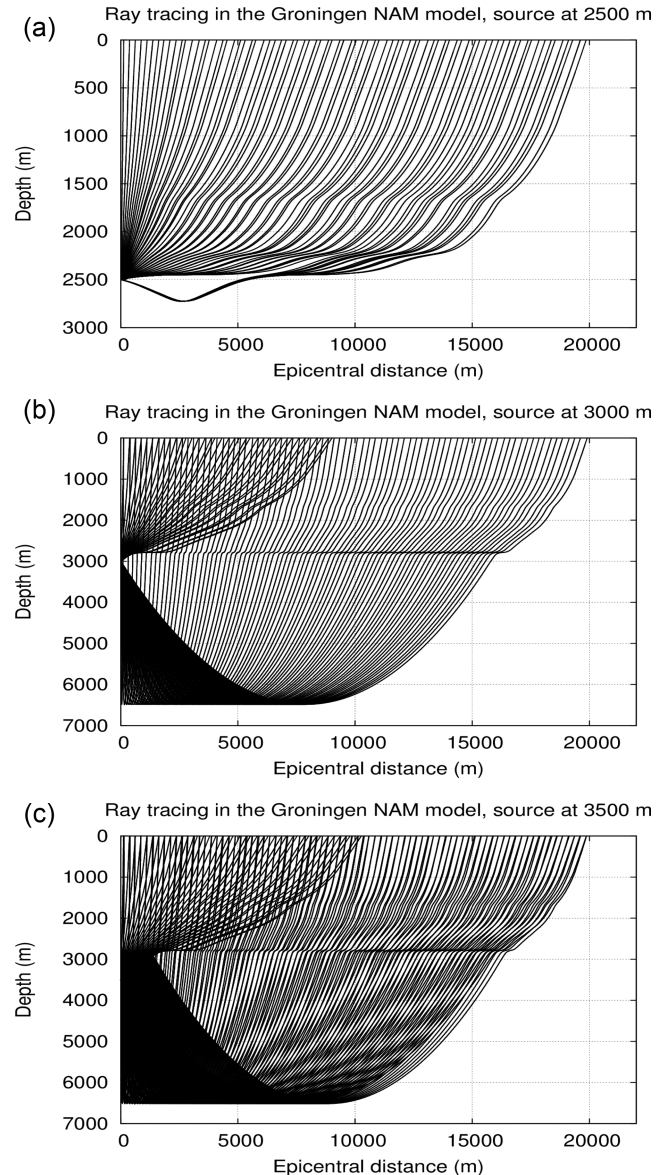
Figure 9. Ray tracing in the complex Groningen subsurface. (a) The source depth is 2500 m. (b) The source depth is 3000 m. (c) The source depth is 3500 m.

direct wavefield is dominant for source depths above the reservoir. On the other hand for source depths at reservoir level or in the underburden, the propagating wavefield consists of direct upgoing waves until an epicentral distance about 10–12 km (depending on the source depth) is reached. For longer epicentral distances, diving waves will arrive at the stations. Several examples of direct and diving waves in event gathers recorded in the dense network have been observed. We refer to the KNMI webpage (http://www.knmi.nl/nederland-nu/seismologie/aardbevingen.html) for examples of events gathers in Groningen.

A regular 3-D grid is used to parametrize the misfit function used in the source location. The number of cells in the grid is 100 × 100 × 31 (AreaxDepth). The coordinates for the surface area in RD-coordinates is limited to [228512; 267512] and [569312; 613712], respectively. The depth range is between 2 and 3.5 km which is where the Zechstein group, Rotliegende gas reservoir and Carboniferous underburden are found.

Travel Time Curves for the Groningen NAM Model
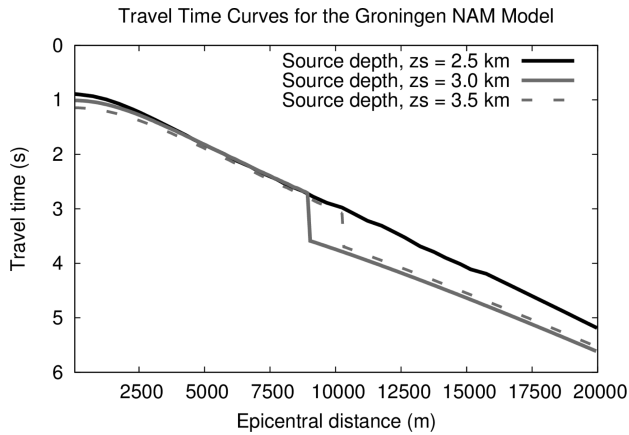
Figure 10. Traveltime curves for a source depth at 2500, 3000 and 3500 m.

The EDT method to determine the source location in Section 4 consists of two steps. The first step is the same for all events in Groningen: (1) An imaginary earthquake is located at the centre of a cell in the 3-D grid. Traveltime curves for the general 1-D velocity profile in Fig. 7 near Loppersum are used to produce estimated differential traveltimes which are compared to the observed data in the misfit function in eq. (4) for all possible station pairs. The minimum point of the misfit function is determined with a global search method (Tarantola 1987) resulting in the first iterative estimate of the event focus. (2) The 1-D velocity model in Fig. 7 is considered to be a too general velocity model for Groningen. The depth resolution of the event in the first iterative focus may therefore still be too inadequate. A second iteration is carried out to get a better idea about the depth of the event. The second step is similar to the first step, except that a new traveltime function is calculated for the local velocity profile at the epicentre coordinates found in the first iteration.

To quantify the improvement of the focus estimation of an event, the root mean squared (rms) value of differential traveltimes is calculated with

$$\text{rms} = \sqrt{\frac{1}{N} \sum_i^N \left[\Delta T_{\text{obs}} - \Delta T_{\text{calc}} \right]^2}. \tag{10}$$

The rms formula in expression (10) is identical to eq. (7) in Satriano *et al.* (2008).

6 RESULTS OF DEPTH ESTIMATION OF INDUCED EARTHQUAKES IN GRONINGEN

Before the year 2014, the original borehole network was not capable to accurately determine the depth of induced events in the region, due to a large average interstation distance (20 km) and a strong lateral variation of the *P*- and *S*-velocities in the upper 4 km of the crust which required the use of average regional velocity models. For the largest recorded event, the M3.6 induced earthquake on 2012 August 16, only three stations were operational within an epicentral distance of 15 km. The epicentre of this event estimated by the EDT method is close to the location reported in the KNMI earthquake catalogue. However, it is rather difficult to give a reliable estimate of the focal depth based on these three data points. For many other events for which the determination of the event was unreliable, the azimuthal coverage was too poor. The depth of events in the KNMI earthquake catalogue is by default 3 km. The station density over

the Groningen gas field started to improve in 2014 when the first new geophone stations were installed. In the year 2015, the station network was further improved, with about 60 borehole stations in Groningen in the second part of the year. Currently, there are about 90 locations with instruments (i.e. three-component geophones and accelerometers) from the old and new network.

A total of 87 events from February 2014 to July 2016 were processed with the two-step EDT method. Three events on 2014 March 15, 2015 June 6 and 2015 July 18 are presented and discussed below. These events were selected based on their location at three different depth intervals. The setup is the same in all figures. The error on the depth is obtained by propagating the discrepancy between observed and calculated traveltime differences for each station pair into the misfit function. Hereby, the total misfit function curve get shifted in the vertical direction. The shift of the minimum point of the misfit function is an indication of the error of the depth. The epicentre location is much less sensitive to errors between the observed − calculated traveltimes.

Results for the event on 2014 March 15 are shown in Fig. 11. All stations used in the procedure are located to the western side of the epicentre. The distance between epicentres calculated with the hypocentre and EDT method is about 1.5 km. The 'petal' pattern of the misfit function illustrates the lateral variability of stations due to the maximum epicentral distance of the pre-calculated traveltime functions. The average over the number of station pairs in eq. (4) takes into account the effect of a variable number of station pairs. The misfit function indicates a depth of the induced earthquake about 2850 m ± 100 m. Note the vertical cross-section of the misfit function is similar to the vertical profile of the misfit function in the synthetic experiment in Fig. 6. The east–west cross-section of the detailed 3-D elastic model together with the estimated focus of the induced earthquake shows that the event took place in the Rotliegend gas reservoir. This result applies to most of the processed events. The depth of the event on 2015 June 6th (Fig. 12) is calculated at 3150 ± 100 m. This is in the lower part of the gas bearing sandstone reservoir or in the underburden. Similar to the second event, the estimated epicentre of the event on 2015 July 18th (Fig. 13) is well-surrounded by stations. The distance between the epicentres determined by the two methods is less than 500 m. The misfit function indicates that the depth of the event is about 2200 ± 150 m. The event location coincides with the upper anhydrite and a graben structure in the Zechstein group. The upper anhydrite layer in the Zechstein layer is much closer to the Rotliegend gas reservoir compared to the neighbouring structure. The anhydrite layers are made of a stiff, brittle material. The magnitude of this event is 0.7 according to the KNMI earthquake catalogue. Other events (i.e. 2015 June 30; 2015 November 9; 2015 November 10; 2015 December 8; 2016 February 25; 2016 July 9) with magnitudes in the range [0.5; 1.1] have also been located in the upper anhydrite layer. Information about the depth and error bars on the depth of induced earthquakes is available in Table 1. From this table, one can see that the epicentre estimated by the hypocentre and EDT method are comparable. The depth range of the events is between 2200 and 3500 m with the majority between 2600 m and 3200 m (i.e. reservoir depth). The error on the depth is often between 100 m and 200 m. Fig. 14 shows the resulting event depth distribution related to the number of events (a), the magnitude (b) and the structural information (c). Most events are centred around 2700–3000 m with several shallow events in the anhydrite layer and others in the underburden. It does seem possible to have induced earthquakes in the overburden with the Zechstein group and in the carboniferous underburden.
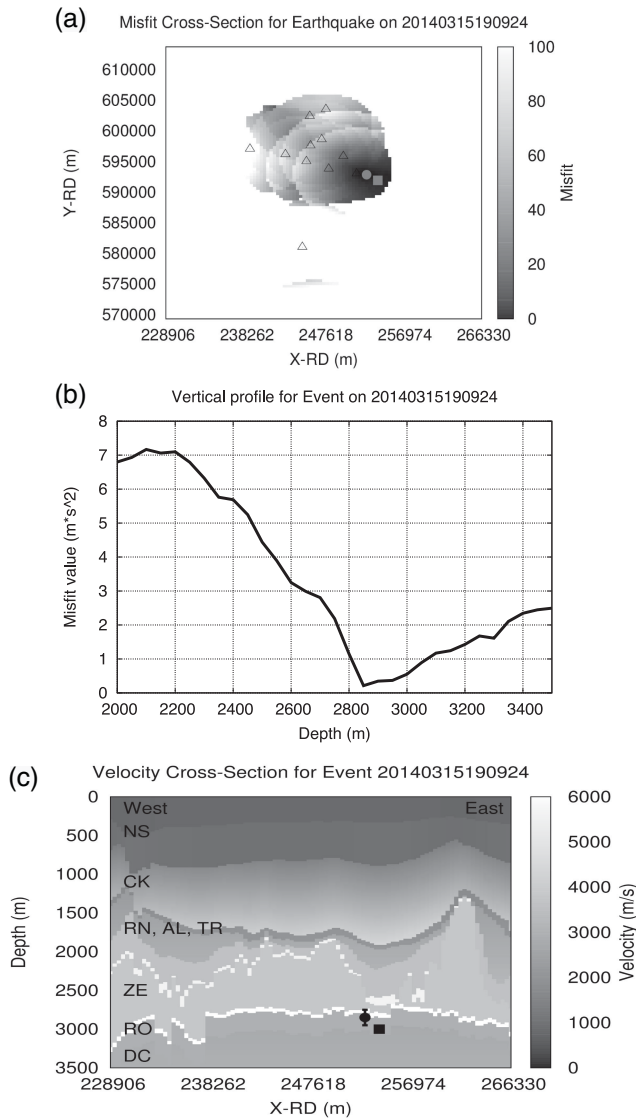
Figure 11. Focus estimation of the event on 2014 March 15 at the time 19h09m24s. (a) The horizontal cross-section of the misfit function at estimated source depth. Stations are plotted with triangles. (b) The vertical cross-section of the misfit function at the estimated surface coordinate. (c) West–east cross-section of the 3-D NAM elastic model with the location of the earthquake. The KNMI hypocentre location is indicated with the filled square while the estimated focus in the EDT method is shown with the filled sphere and vertical error bar.

With respect to the magnitudes, the trend is clear. Generally, induced earthquakes at the shallow anhydrite layer within the Zechstein group have a small magnitude less than 1.0, while events at reservoir level can be weak as well as stronger. Remember that the station network was recently extended which has contributed with more recordings of induced earthquakes with magnitudes lower than 1.5. One possible explanation for the overburden events in the upper stiff anhydrite layer with a thickness about 30–50 m (van Gent *et al.* 2011), may be the increase in horizontal stress above the compacting reservoir, which may lead to movements along existing fractures in the anhydrite layer.

The structure of the Rotliegend gas reservoir in Groningen varies laterally. For an illustration of the gas reservoir structure, we refer to Fig. 3. At the reservoir boundaries (i.e. north, east, south and
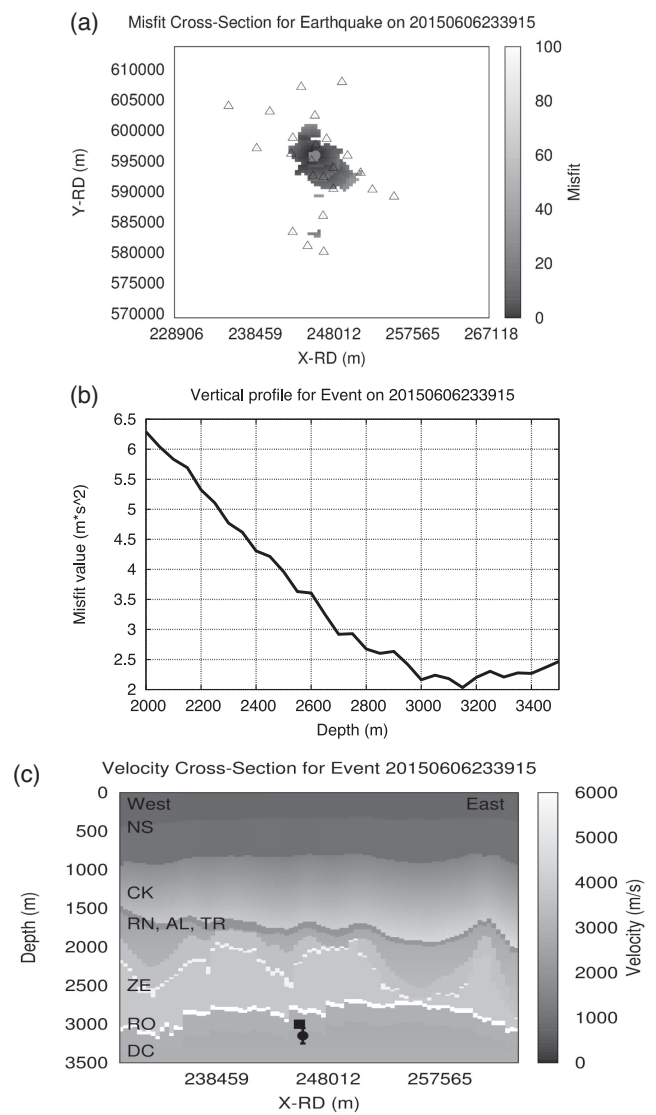
Figure 12. Focus estimation of the event on 2015 June 6 at the time 23h39m15s. Identical setup as in Fig. 11.

west), the reservoir is deeper, while close to Loppersum in the central part of Groningen the reservoir is somewhat more shallow. By visual inspection, the structural location (i.e. upper anhydrite layer, reservoir and underburden) of all events was determined. The histogram in Fig. 14 shows the distribution of the structural location of the induced earthquakes. The majority of the events are found at reservoir level. A small number of induced events (with the current data estimated to be less than 10 per cent) are located in the upper anhydrite layer (i.e. top floater) or in the underburden.

In the year 2014, NAM installed two deep boreholes at 3 km depth in the reservoir in the Loppersum area near the villages Stedum and Zeerijp. The wells are equipped with 3-component geophones at reservoir level. The lateral distance between the two wells is 3 km. Local micro seismicity is reported and analysed by NAM. Focal depth estimates of recorded induced earthquakes are ranging between 2400 and 3200 m with a cluster of events at reservoir level between 2800 and 3100 m (Pickering 2015). By visual inspection of the magnitude distribution, it can be seen that events with a magnitude above one are mainly between 2800 and 3000 m (i.e. reservoir depth).

(a)

(b)

(c)
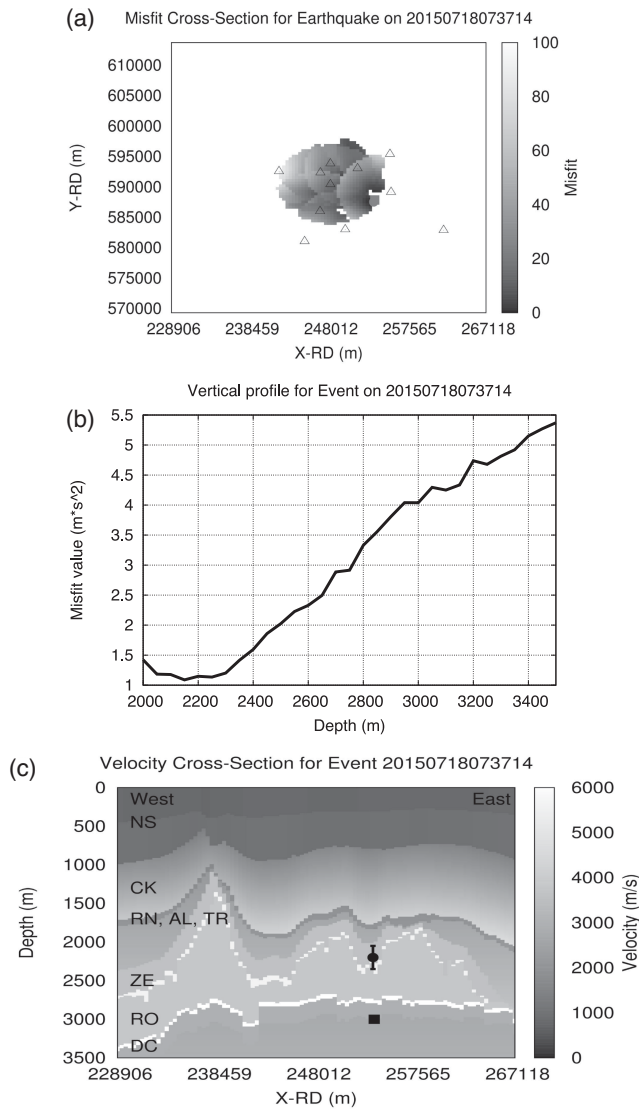
Figure 13. Focus estimation of the event on 2015 July 18 at the time 7h37m14s. Identical setup as in Fig. 11.

A comparison of the epicentres calculated using the hypocentre and EDT method of all the processed induced earthquakes is shown in Fig. 15. The fault structure and the coast lines of the province of Groningen are included in the figure. The estimated epicentres by both methods seem to follow two main lines on the NW–SE aligned fault system. One trendline of events is more towards to the city Delfzijl and the other one is shifted towards the city Groningen. The epicentres by the hypocentre and the EDT method are often located on or near a fault. We are well aware of the possibility that there are mapped and unmapped faults in the current fault model. For several events, the epicentre estimated by the two methods may not necessarily correlate with the same fault. Most epicentre solutions for the same event differ less than 1 km.

7 CONCLUSIONS

Due to the installation of a new dense borehole network, a sub-set of the hydrocarbon induced earthquakes recorded in the province of Groningen (The Netherlands) has been relocated. Especially the depth of the events, which was fixed to 3 km in the original location

(a)

(b)

(c)
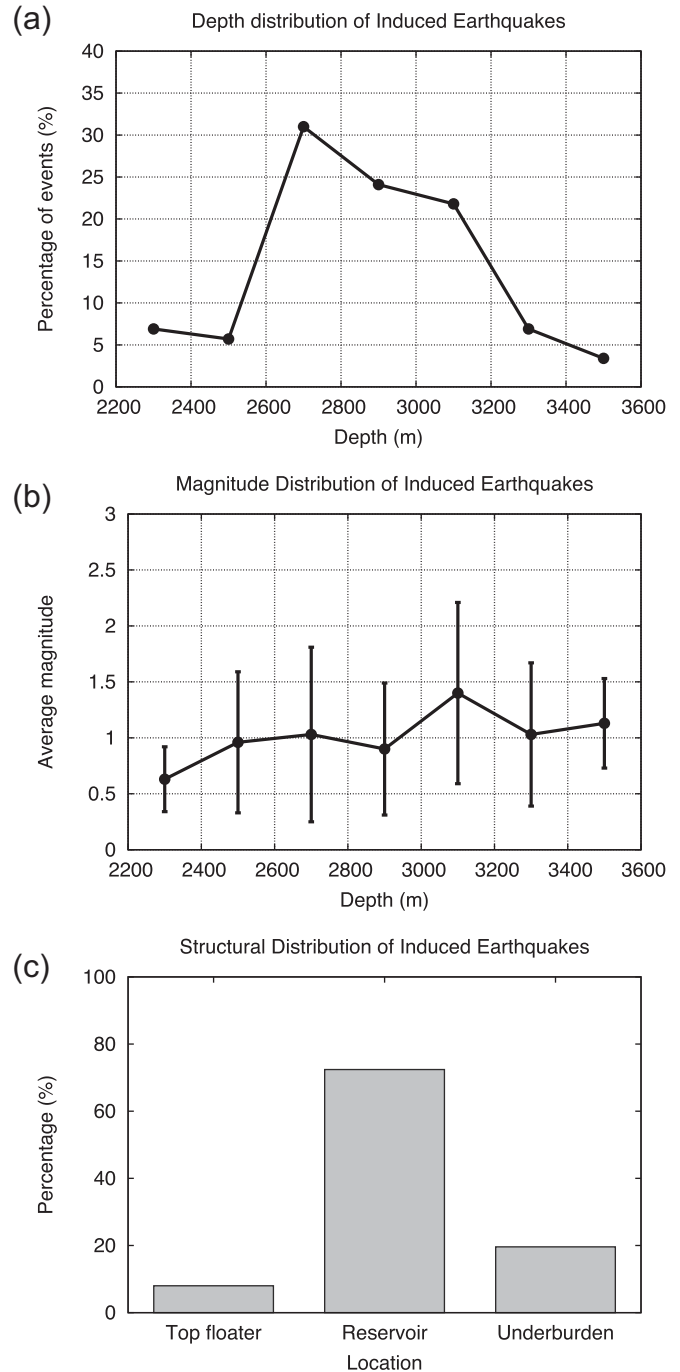
Figure 14. Simple statistical analysis of the assessed induced earthquakes. (a) Depth distribution. (b) Magnitude distribution. (c) Structural distribution.

procedure, could be calculated with an average resolution of 100–200 m. Besides the new network, the availability of a detailed 3-D velocity model and a new location method were essential to obtain these results.

A differential traveltime approach similar to the EDT method (Lomax 2005; Theunissen *et al.* 2012) was applied to the hypocentre estimation of the induced earthquakes in Groningen. Instead of defining a misfit function based on the traveltime residuals for single stations, the residual of differential traveltimes between stations is used in the objective function. The total misfit function is obtained by summing the contributions of differential traveltimes residuals

Table 1. Source locations obtained with the KNMI hypocentre and the EDT method. RD coordinates are used for the epicentre location. The errors for the depth estimate in the EDT method are indicated.

Event date	Magnitude	Hypocentre method x (m)	y (m)	EDT method x (m)	y (m)	z (m)	Vertical error (m)
20140213021314	3.0	247804	597489	246842	596840	3100	100
20140218050332	1.7	239854	595190	238652	595064	3200	100
20140315190924	1.9	254023	591918	252692	592844	2850	100
20140318211518	2.1	236868	600981	237872	599948	2750	200
20141230023736	2.8	244601	581022	244502	581300	2700	100
20150106065528	2.7	247027	593926	246842	593732	3150	150
20150204223447	1.1	251236	594509	250742	595064	3300	300
20150225100256	2.3	252914	593969	255252	594620	2700	200
20150516141449	1.6	252285	592100	252302	591956	2700	100
20150606233915	1.9	245771	595702	246062	595952	3150	100
20150610022607	1.8	245963	596151	245672	595952	3250	250
20150610142127	0.8	243297	596212	243722	596840	2800	250
20150630005300	0.5	241571	588500	241772	588848	2400	200
20150704180758	1.1	242019	596857	242162	596840	2700	200
20150718073714	0.7	253595	587841	253472	587516	2200	150
20150718234729	0.5	246816	579358	246842	579524	2500	100
20150721021804	1.3	249319	594880	249572	594620	2900	100
20150730153452	0.7	247571	578371	248402	579524	2650	100
20150818070612	2.0	246365	578459	246062	579080	2850	100
20150822001230	1.4	246365	578459	244892	584852	3050	100
20150828080727	1.3	251120	581446	250352	582188	2800	100
20150905033430	0.5	244594	576645	244892	577304	2850	100
20150909200151	1.2	242754	582176	244112	583076	2550	200
20150930180537	3.1	251603	584016	251522	584408	3200	200
20151009002719	0.3	251531	590916	251522	590180	3050	100
20151010055148	0.2	249281	586641	250352	586628	2950	200
20151011044142	0.3	253016	576920	253082	577304	2700	100
20151027154628	1.2	245818	593254	246452	594176	3150	300
20151030160718	1.7	247535	590615	247232	590180	2600	250
20151030184901	2.3	257224	589810	255812	588848	2700	100
20151109131737	0.7	259445	585850	258932	585296	2300	300
20151110163223	0.6	249130	584078	251522	584852	2500	100
20151112123009	0.6	243045	580846	244892	582188	2800	100
20151202064002	1.6	251725	584575	251132	585296	2750	200
20151208035422	0.8	240451	595159	240212	594620	2200	200
20151215000150	1.6	255247	595000	255032	595508	2550	100
20151215074355	1.7	236168	588406	235922	589292	3250	250
20160102000428	0.5	241189	591164	241382	590624	3150	200
20160107052555	1.6	250413	576645	249962	576860	3050	300
20160111053135	0.6	250309	578535	250352	578636	3150	300
20160113064142	1.3	252973	585602	252692	585740	2750	250
20160117115733	1.5	251950	586694	251522	586628	3000	200
20160119131907	0.6	247056	598175	246842	597728	2900	300
20160126222233	1.5	244056	580419	243722	580412	3450	200
20160217002052	0.9	259523	585295	259322	585296	2950	400
20160218081444	0.4	245035	592348	245282	592400	2750	150
20160219030421	0.1	245553	593137	245672	593732	2800	100
20160219214837	1.3	237065	586640	237092	587072	3150	100
20160220034458	0.7	237551	597223	237482	597284	3450	200
20160221050914	0.2	245001	597691	244892	597728	3350	200
20160225222630	2.4	248172	578382	248012	578192	2800	100
20160229011957	0.3	247976	578156	248012	578192	2200	100
20160303195429	0.2	247556	579150	248402	579524	2650	100
20160304130029	0.9	241378	599182	241382	599060	3350	300
20160307101653	1.2	250993	587788	251132	587516	2900	250
20160309225107	0.4	251986	581574	251912	581744	2850	200
20160311113323	0.9	251617	580009	251912	580412	3050	250
20160316145802	0.5	248734	587299	249182	587072	3250	250
20160320220213	0.5	252759	586266	252692	586628	2800	200
20160325012659	1.8	256270	574872	256202	575084	3000	350
20160325094639	0.7	238965	584892	239822	585740	3200	200
20160331133342	0.7	237517	587538	237872	587960	2750	100
20160402004753	1.1	239756	585462	239822	585740	2800	150

Table 1 – *continued*

Event date	Magnitude	Hypocentre method		EDT method			
		x (m)	y (m)	x (m)	y (m)	z (m)	Vertical error (m)
20160404181249	0.5	235560	592805	239432	592400	3000	150
20160409174557	0.3	247533	590726	248012	590624	3000	300
20160413110045	0.7	259789	588418	259322	589292	2850	150
20160424065858	0.4	252611	590270	252692	590180	2450	100
20160424153647	1.1	251009	583670	251522	583964	2950	150
20160511071133	0.4	233465	590476	233192	591512	3000	200
20160515115715	1.0	261867	588018	261272	587960	3200	300
20160516203841	1.1	256943	590471	256202	590180	3050	100
20160516222437	0.4	256223	589788	256592	590180	2800	100
20160528020820	1.2	238310	584101	239042	584408	3050	250
20160529142754	1.1	251553	589803	251522	589736	2900	150
20160601080254	1.2	245727	598039	245672	597728	3450	300
20160602184313	1.5	257576	585809	256982	585740	2950	200
20160616005616	0.3	241404	582931	240212	584408	2950	100
20160616032708	0.5	251543	583681	251522	584408	2700	150
20160618111046	0.1	249024	596321	249182	596396	2950	150
20160618235825	1.2	247169	578363	247232	579080	2750	300
20160622131010	0.7	249825	596226	248792	595952	2750	100
20160706215400	0.3	239783	595258	239432	595508	2650	100
20160709104753	1.1	248679	572938	247622	574640	2350	100
20160717120118	0.5	255262	578302	255032	578636	2800	150
20160718085811	1.7	242963	599880	243332	599060	3100	400
20160722105515	0.3	252901	589163	253472	590624	2850	100
20160723175945	0.1	255911	582434	256202	582632	2700	100
20160726140210	0.9	256376	588901	256592	589292	2900	100
20160728053213	0.3	253232	589281	252692	589292	3200	300
20160728155728	0.8	250900	585783	251132	586184	3100	300
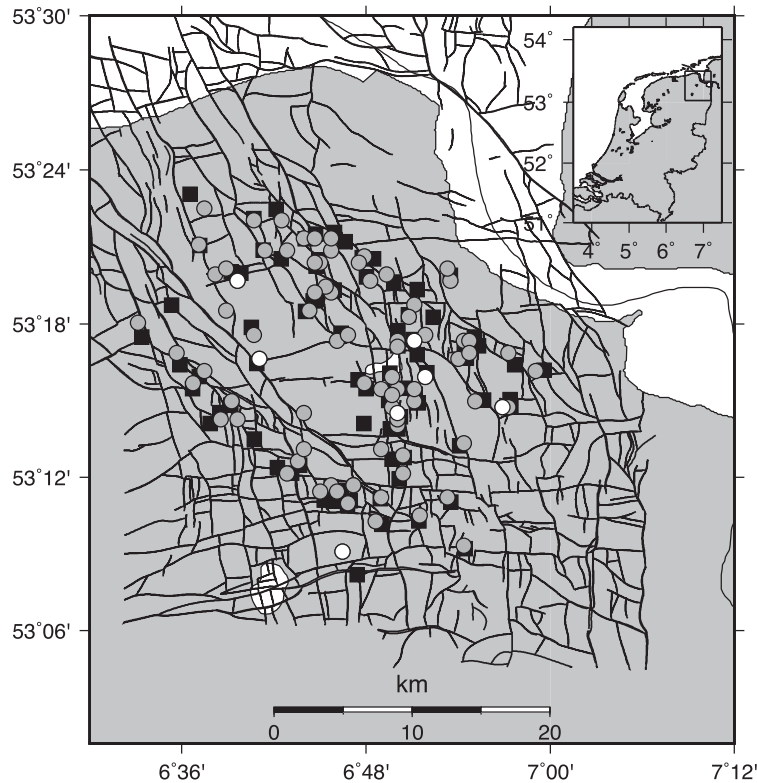
Figure 15. Map of the province of Groningen with epicentres estimated with the hypocentre method and the EDT approach for selected events from 2014 to July 2016. The black squares indicate epicentres from the hypocentre method. The epicentres at reservoir level and in the floater as estimated in the differential traveltime method are shown with a grey and white filled circle, respectively. The square and circle closest to each other are derived from the same induced earthquake. The NW–SE aligned fault system is illustrated with black lines.

from all station-pairs for one event. By minimizing the misfit function by means of a standard global search method, the hypocentre of the event and the uncertainty in the depth parameter are calculated.

As a rule of thumb, at least 3–4 stations with epicentral distances shorter than 5–8 km must be available in order to obtain an estimate of the event depth. The epicentre is much easier to measure even when applying stations located farther away or the azimuthal coverage is poor.

The EDT method was applied on 87 induced earthquakes from 2014 to July 2016. For earlier events recorded before 2014, the station network was too sparse. Most of the located events are found at reservoir level. Several events with a magnitude about 0.5–1.1 are found near a stiff anhydrite layer in the Zechstein group. It is observed that the magnitude of the events is weaker in the overburden while a range of weak to moderate events take place in the reservoir compartment and uppermost part of the underburden. A possible explanation for the anhydrite events can be the increase in horizontal stress above the compacting reservoir, which may lead to movements along existing fractures in the anhydrite layer. The estimated epicentres for events at reservoir level correlate well with the mapped fault system in Groningen.

The developed method for hypocentre location of induced earthquakes will be applied to future recorded events in Groningen. It is expected that the EDT method will soon be implemented as a module in the automatic location program (seisComP3 by Gzf and Gempa). The database of induced events is an essential ingredient for hazard and risk studies (Bommer *et al.* 2016).

ACKNOWLEDGEMENTS

REFERENCES

Aki, K. & Richards, P.G., 1980. *Quantitative Seismology, Theory and Methods,* Freeman and Company.

Bommer, J.J., Dost, B., Edwards, B., Stafford, P.J., van Elk, J., Doornhof, D. & Ntinalexis, M., 2016. Developing an application-specific ground-motion model for induced seismicity, *Bull. seism. Soc. Am.,* **106,** 158–173.

Bourne, S.J., Oates, S.J., Bommer, J.J., Dost, B., van Elk, J. & Doornhof, D., 2015. A Monte Carlo method for probabilistic hazard assessment of induced seismicity due to conventional natural gas production, *Bull. seism. Soc. Am.,* **105,** 1721–1738.

Dalfsen, W., Doornenbal, J.C., Dortland, S. & Gunnink, J.L., 2006. A comprehensive seismic velocity model for The Netherlands based on lithostratigraphic layers, *Neth. J. Geosci.,* **85**(4), 277–292.

Dino loket, Available at: http://www.dinoloket.nl, last accessed 2 February 2017 (Database with geological information, website from TNO).

Dost, B. & Haak, H.W., 2007. Natural and induced seismicity, in Geology of the Netherlands, pp. 223–229, eds Wong, Th.E., Batjes, D.A.J. & de Jager, J., Royal Netherlands Academy of Arts and Sciences.

Dost, B. & Kraaijpoel, D., 2013. *The August 16, 2012 Earthquake Near Huizinge (Groningen),* KNMI Publication.

Duin, E.J.T., Doornenbal, J.C., Rijkers, R.H.B., Verbeek, J.W. & Wong, Th.E., 2006. Subsurface structure of The Netherlands - results of recent onshore and offshore mapping, *Neth. J. Geosci.,* **85**(4), 245–276.

Font, Y., Kao, H., Lallemand, S., Liu, C.S. & Chiao, L.Y., 2004. Hypocentral Determination Offshore Eastern Taiwan using the Maximum Intersection Method, *Geophys. J. Int.,* **158,** 655–675.

Kennett, B.L.N., 1993. *Seismic Waves Propagation in Stratified Media,* Cambridge Univ. press.

Kraaijpoel, D. & Dost, B., 2013. Implications of salt-related propagation and mode conversion effects on the analysis of induced seismicity, *J. Seismol.,* **17,** 95–107.

Lienert, B.R., Berg, E. & Frazer, L.N., 1986. Hypocenter: an earthquake location method using centered, scaled, and adaptively damped least squares, *Bull. seism. Soc. Am.,* **76,** 771–783.

Lomax, A., 2005. A Reanalysis of the hypocentral location and related observations for the Great 1906 California earthquake, *Bull. seism. Soc. Am.,* **95,** 861–877.

NLog, Available at: http://www.nlog.nl, last accessed 2 February 2017 (Netherlands Oil and Gas Portal, website from TNO).

Pickering, M., 2015. An estimate of the earthquake hypocenter locations in the Groningen Gas Field, NAM Publication, 95 pp. (http://feitenencijfers.namplatform.nl/download/rapport/8b16a9eb-a607-494a-baa5-56e349b6ed0c?open=true)

Robertson, J.O.A., Blanch, J.O. & Symes, W.W., 1994. Viscoelastic finite-difference modeling, *Geophysics,* **59,** 1444–1456.

Satriano, C., Lomax, A. & Zollo, A., 2008. Real-Time evolutionary earthquake location for seismic early warning, *Bull. seism. Soc. Am.,* **98,** 1482–1494.

Snieder, R., 2004. *A Guided Tour of Mathematical Methods,* Cambridge Univ. Press.

Tarantola, A., 1987. *Inverse Problem Theory: Methods for Data Fitting and Model Parameter Estimation,* Elsevier.

Theunissen, T., Font, Y., Lallemand, S. & Gautier, S., 2012. Improvements of the maximum intersection method for 3D absolute earthquake locations, *Bull. seism. Soc. Am.,* **102,** 1764–1785.

Van Gent, H., Ural, J. & de Keizer, M., 2011. The internal geometry of salt structures–a first look using 3D seismic data from the Zechstein of the Netherlands, *J. Struct. Geol.,* **33,** 292–311.

Waldhauser, F. & Ellsworth, W.L., 2000. A double-difference earthquake location algorithm: method and application to the Northern Falut, California, *Bull. seism. Soc. Am.,* **90,** 1353–1368.

Zhang, H. & Thurber, C., 2006. Development and application of double-difference seismic tomography, *Pure appl. Geophys.,* **163,** 373–403.